VORTEX SHEDDING SUPPRESSION ON A BLUFF BODY IN THE VICINITY OF A MOVING GROUND

Alex Mendonça Bimbato, alexbimbato@unifei.edu.br
Luiz Antonio Alcântara Pereira, luizantp@unifei.edu.br
Institute of Mechanical Engineering, Federal University of Itajuba, Itajuba, CP 50, Minas Gerais, Brazil

Miguel Hiroo Hirata, hirata@superonda.com.br
State University of Rio de Janeiro, FAT-UERJ, Resende, Rio de Janeiro, Brazil

Abstract. *The present work deals with the Vortex Method to study the vortex shedding suppression which occurs when a circular cylinder is placed near a plane surface that moves with the same velocity as the incident flow; this situation is particular important in practical engineering problems since it works with relative motion. Experimental data available in the literature show that in this kind of flow there is practically no boundary layer developed on the ground surface; using these observations in this work the ground plane motion is represented by the absence of vorticity generation on it. The numerical results obtained show that the above numerical strategy represented successfully the vortex shedding suppression.*

Keywords*: Vortex Method, Ground Effect, Moving Ground, Vortex Shedding Suppression.*

1. INTRODUCTION

The flow around bluff bodies causes interesting fluid dynamics phenomena such as separation, vortex shedding and turbulence transition; the vortex shedding mechanism has been studied frequently since it affects many fluid dynamic properties like drag and lift forces, vortex induced vibration, noise and heat and mass transfer efficiency. A particular interesting situation occurs when a circular cylinder is close to a plane boundary; in this case it can be observed that as the cylinder comes close to the ground the vortex shedding frequency decreases until its suppression what means that the gap between the cylinder and the ground, h, characterized by the gap-ratio h/d (d is cylinder diameter), is an influential parameter.

One of the first researches that investigate the influence of the distance between the cylinder and the ground was made by Taneda (1965) in a water tunnel at $Re = 170$. In this test the ground had the same speed as the water flow (moving ground configuration) and Taneda (1965) observed a decrease on the vortex shedding frequency when the gap ratio was less than 0.1.

Bearman and Zdravkovich (1978) performed velocity measurements to study the vortex shedding frequency when the circular cylinder is close to a fixed ground at $Re = 4.8 \times 10^4$. The authors verified a constant value for the Strouhal number (a dimensionless parameter used to measure the vortex shedding frequency), $St \cong 0.2$, for any $h/d < 0.3$.

Contradicting the results of Bearman and Zdravkovich (1978), Buresti and Lanciotti (1979) measured the Strouhal number when the cylinder is near to a fixed ground at $Re = 1.9 \times 10^5$ and found a critical gap-ratio (h/d_c) of 0.4 and a Strouhal value about 0.2 when $h/d > 0.4$. Therefore the critical gap-ratio and the Strouhal number depend on the flow regime and it seems to be impossible to define exact values for these variables. However it can be stated that for high Reynolds number flows the Strouhal number decreases as the gap-ratio decreases.

Nishino (2007) studied drag and lift coefficients acting on a circular cylinder placed near a moving ground at $Re = 4.0 \times 10^4$ and $Re = 1.0 \times 10^5$; the ground had the same speed as the air flow. In this experimental configuration the author observed that practically no boundary layer was developed on the ground surface and found three ranges of gap-ratio where important phenomena happen: (a) if $h/d > 0.50$, larger vortex structures are generated at the rear part of the cylinder; (b) if $0.35 < h/d < 0.50$ the vortex shedding is intermittent; (c) if $h/d < 0.35$ the vortex shedding is suppressed. Nishino (2007) also studied the end effects on the aerodynamic loads behaviour using end-plates, making possible comparisons between two-dimensional and three-dimensional flows.

The present work uses a two-dimensional Lagrangian Vortex Method to analyse the vortex shedding suppression that happens when a circular cylinder is close to a moving ground at subcritical Reynolds number ($Re = 1.0 \times 10^5$).

The Vortex Method used in this work discretizes the vorticity present in the fluid domain using discrete vortices which are followed individually throughout the numerical simulation. As a consequence it is a mesh-free method and the governing equations are solved only where vorticity is present; thus the far away boundary condition is automatically satisfied. The previously mentioned advantages make the Discrete Vortex Method capable to be applied for the analysis of complex, unsteady and vortical flows; some of the most important works using the Vortex Method are: Chorin (1973), Leonard (1980), Sarpkaya (1989), Lewis (1991), Kamemoto (2004).

Considering the conclusions obtained by Nishino (2007), since there is practically no boundary layer developed on the ground (once the ground has the same velocity as the free stream), in the present work the moving ground is represented by the absence of vorticity generation on the ground, what means that the ground surface remains fixed. This numerical strategy was successfully used by Bimbato *et al*. (2011).

2. GOVERNING EQUATIONS

Figure 1 schematically represents the two-dimensional, incompressible and unsteady viscous flow around a circular cylinder placed near a surface (the ground surface) whose movement is represented by the absence of vorticity generation according to Bimbato *et al*. (2011); $U = 1$ is the free stream velocity, $d = 1$ is the cylinder diameter, h/d is the distance between the circular cylinder and the ground plane (the gap-ratio), Ω is the fluid domain defined by $S = S_1 \cup S_2 \cup S_3$ where S_1 is the body surface, S_2 is the ground surface and S_3 is defined far away.

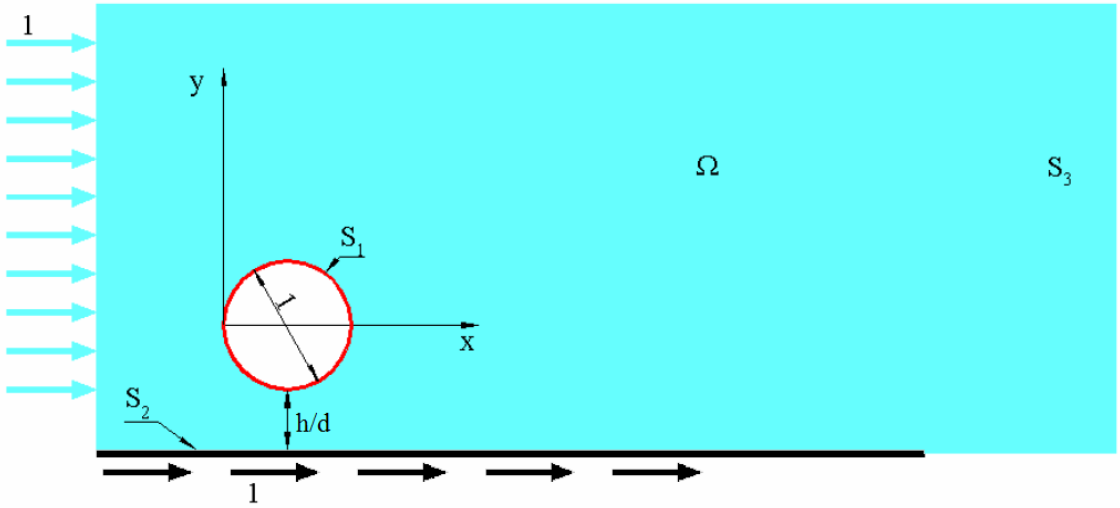

Figure 1. Definition of fluid region.

The studied phenomenon is governed by the continuity and the Navier-Stokes equations, which can be written:

$$\nabla \cdot \boldsymbol{u} = 0 \tag{1}$$

$$\frac{\partial \boldsymbol{u}}{\partial t} + \boldsymbol{u} \cdot \nabla \boldsymbol{u} = -\frac{1}{\rho}\nabla p + \frac{\mu}{\rho}\nabla^2 \boldsymbol{u} \tag{2}$$

where $\boldsymbol{u}$ is the velocity vector, ρ is the density, p is the pressure field and μ is dinamic viscosity.

It is necessary to impose the boundary conditions. The impenetrability condition (Eq. (3)) demands that the normal velocity component of the fluid particle (u_n) should be equal to the normal velocities components of the surfaces S_1 and S_2 (v_n); on the other hand, the no-slip condition (Eq. (4)) demands that the tangential velocity component of the fluid particle (u_τ) should be equal to the tangential velocity component of the surface S_1 (v_τ), since there is no discrete vortex been generated on S_2 (Bimbato *et al*., 2011). Thus:

$$u_n - v_n = 0, \text{ on } S_1 \text{ and } S_2 \tag{3}$$

$$u_\tau - v_\tau = 0, \text{ only on } S_1 \tag{4}$$

Finally, one assumes that, far away, the perturbation caused by the body and the ground plane fades as:

$$|\boldsymbol{u}| \to U \text{ on } S_3 \tag{5}$$

3. SOLUTION METHOD

Taking the curl of Eq. (2) and considering Eq. (1), Batchelor (1967) obtained the 2-D vorticity equation:

$$\frac{\partial \omega}{\partial t} + \boldsymbol{u} \cdot \nabla \omega = \frac{1}{Re} \nabla^2 \omega \tag{6}$$

In order to simplify the numerical implementation of the Vortex Method, Chorin (1973) proposed the "Viscous Splitting Algorithm" to separate the vorticity convection (Eq.(7)) from the vorticity diffusion (Eq.(8)). Thus:

$$\frac{D\omega}{Dt} = \frac{\partial \omega}{\partial t} + (\boldsymbol{u} \cdot \nabla)\omega = 0 \tag{7}$$

$$\frac{\partial \omega}{\partial t} = \frac{1}{Re} \nabla^2 \omega \tag{8}$$

where $D\omega/Dt$ indicates the lagrangian description.

In order to solve vorticity convection the velocity field must be calculated in the position of each discret vortex *j* present in the fluid domain, which is composed by three contributions: (i) the incident flow, $ui(\boldsymbol{x},t)$; (ii) the solid boundaries, $ub(\boldsymbol{x},t)$; (iii) the vortex-vortex interaction, $uv(\boldsymbol{x},t)$.

The velocity induced by the incident flow is given by:

$$ui_1 = 1 \quad and \quad ui_2 = 0 \tag{9}$$

The present work deals to the Panel´s Method (Katz and Plotkin, 1991) to represent the solid boundaries. For this purpose, the circular cylinder and the ground plane are discretized by source flat panels with constant density. Thus, the velocity induced by the solid boundaries in the position of *j* discrete vortex is given by:

$$ub_i(x_j,t) = \sum_{k=1}^{NP} \psi_k c_{jk}^i \left(x_j(t) - x_k\right), \; i = 1,2 \text{ and } j = 1,Z \tag{10}$$

where, *NP* is the total number of source flat panels, $\psi_k = const$ is the source density per unit length and $c_{jk}^i\left[\boldsymbol{x}_j(t) - \boldsymbol{x}_k\right]$ is the *i* component of the velocity induced at discrete vortex *j* by *k* panel.

Finally, the vortex cloud contribution is given by:

$$uv_i(x_j,t) = \sum_{k=1}^{Z} \Gamma_k c_{jk}^i \left[x_j(t) - x_k(t)\right], \; i = 1,2 \text{ and } j = 1,Z \tag{11}$$

where Γ_k is the intensity of the *k* vortex and $c_{jk}^i\left[\boldsymbol{x}_j(t) - \boldsymbol{x}_k(t)\right]$ is the *i* component of the induced velocity in a discrete vortex *j* by a *k* discrete vortex.

With the velocity field, Eq. (7) is solved using a first order Euler scheme (Ferziger, 1981):

$$\boldsymbol{x}_j(t + \Delta t) = \boldsymbol{x}_j(t) + \boldsymbol{u}_j(\boldsymbol{x},t)\Delta t \;, j=1, Z \tag{12}$$

where Δt is the time increment of the numerical simulation.

Ultimately, to completely solve the 2-D vorticity equation is necessary to deal with the diffusion equation. The most common method to take into account the vorticity diffusion with the Vortex Method is the Random Walk Method (Lewis, 1991), which is used in this work. This simple method requires simultaneous radial and circumferential displacements for each discrete vortex such as:

$$\chi_j(\chi_{1j}, \chi_{2j}) = \sqrt{\frac{4\Delta t}{Re} ln\left(\frac{1}{P}\right)}\left[cos(2\pi Q) + isen(2\pi Q)\right] \tag{13}$$

where *P* and *Q* are random numbers with $0 < P < 1$ and $0 < Q < 1$.

Finally, with the vorticity and velocity fields it is possible to compute the pressure field. Kamemoto (1993) used a Bernoulli function defined by Uhlman (1992) and starting from Navier-Stokes equations was able to write a Poisson

equation for the pressure; this equation was solved using a finite difference scheme. Here the same Poisson equation was derived and its solution was obtained through the following integral formulation (Shintani and Akamatsu, 1994):

$$H\overline{Y}_i - \int_{S_1+S_2} \overline{Y}\nabla\Xi_i \cdot \boldsymbol{e}_n dS = \iint_{\Omega} \nabla\Xi_i \cdot (\boldsymbol{u}\times\boldsymbol{\omega}) d\Omega - \frac{1}{Re}\int_{S_1} (\nabla\Xi_i \times \boldsymbol{\omega})\cdot \boldsymbol{e}_n dS \tag{14}$$

where i is the point where the pressure is computed, $H = 1.0$ in the fluid domain, $H = 0.5$ on the boundaries, Ξ is a fundamental solution of Laplace equation and $\boldsymbol{e}_n$ is the unit vector normal to the solid surfaces.

The drag and lift coefficients are expressed by:

$$C_D = \sum_{k=1}^{NP} 2\left(p_k - p_{\infty}\right)\Delta S_k \sin\beta_k = \sum_{k=1}^{NP} C_p \Delta S_k \sin\beta_k \tag{15}$$

$$C_L = -\sum_{k=1}^{NP} 2\left(p_k - p_{\infty}\right)\Delta S_k \cos\beta_k = -\sum_{k=1}^{NP} C_p \Delta S_k \cos\beta_k \tag{16}$$

where p_{∞} is the reference pressure (at S_3), ΔS_k is the length and β_k is the angle and both of the k panel.

4. NUMERICAL SIMULATION OF THE FLOW AROUND A CIRCULAR CYLINDER

4.1. Isolated Circular Cylinder

In order to study the vortex shedding suppression phenomenon which occurs, among other situations, when a circular cylinder is placed near a moving ground, it is convenient to understand the vortex shedding phenomenon in an isolated circular cylinder.

Table 1 shows the comparison between the present results with the experimental ones made by Blevins (1984). In numerical experiments, the circular cylinder is discretized in $NP = 300$ source flat panels, the time increment of the numerical simulations is $\Delta t = 0.05$, the Lamb vortex core is $\sigma_0 = 0.001$ and the Reynolds number is $Re = 1.0\times10^5$.

Table1. Mean values of drag and lift coefficients and Strouhal number of an isolated circular cylinder.

$\mathrm{Re} = 1.0\times10^5$	$\overline{\mathrm{C}}_{\mathrm{D}}$	$\overline{\mathrm{C}}_{\mathrm{L}}$	$\overline{\mathrm{St}}$
Blevins (1984) ± 10%	1.20	-	0.19
Present Simulation	1.210	-0.003	0.216

The mean values are computed after the numerical transient is reached, between $50.00 \le t \le 100.00$ and agree well with the experimental results obtained by Blevins (1984) which is 10% of uncertainty. The Strouhal number, which is a dimensionless parameter that represents the frequency of vortex structures shedding is about *0.21* and is defined as:

$$St = \frac{fd}{U} \tag{17}$$

where f is the frequency of vortex structures shedding.

Since the flow around a circular cylinder is well predicted, the computational code is considered able to simulate the situation where the cylinder suffers the influence of a plane boundary; more details of the study of the flow around an isolated circular cylinder is discussed in Bimbato *et al.* (2011).

4.2. Circular Cylinder near a Moving Ground

The first mechanism that governs the ground effect phenomenon is the wake interference effect which consists of the interference between the wake formed behind the body and the boundary layer developed on the ground. The purpose of using a moving ground is to eliminate the discussed interference which is probably one of the most crucial mechanisms that governs the physics involved in the ground effect problem but that makes its understanding difficult.

The present work deals with the Vortex Method to simulate numerically the two-dimensional, unsteady and viscous flow around a circular cylinder in the vicinity of a moving ground using the same numerical parameters validated in Section 4.1. It is important to emphasize that the main purpose of this work is to study the vortex shedding suppression. The analysis starts with Tab. 2, which shows that the end effects are very significant. The experimental data obtained by

Nishino (2007) show that for $h/d > 0.40$ the longer the flow is two-dimensional, i.e., the greater y_e/d (where y_e/d is the distance between the end-plate border and the circular cylinder), the higher the values of the drag force (compare the drag force values, for a given h/d, when $y_e/d = 0.0$, $y_e/d = 0.2$ and $y_e/d = 0.4$). This happens because in three-dimensional flows there is momentum changes in the axial direction and then the drag force falls; besides it can be observed large differences in the drag force between approximately two-dimensional flows (when the end-plates are used) and three-dimensional ones (when the end-plates are not used). Still as h/d decreases ($h/d < 0.40$) the drag force computed with the end-plates tends to the value of three-dimensional configuration, what means the end-plates lose their ability to make the flow two-dimensional when the body is close to the ground. It can be inferred also the importance of the three-dimensional effects so it can be classified as the second mechanism that governs the ground effect phenomenon.

Table 2. Summary of results for drag and lift coefficients on the flow around a circular cylinder near a moving ground.

h/d	Nishino (2007) – three-dimensional		Nishino (2007) ($y_e/d = 0.0$)		Nishino (2007) ($y_e/d = 0.2$)		Nishino (2007) ($y_e/d = 0.4$)		Present Simulation - two-dimensional		
	$\overline{C}_D$	$\overline{C}_L$	$\overline{C}_D$	$\overline{C}_L$	$\overline{C}_D$	$\overline{C}_L$	$\overline{C}_D$	$\overline{C}_L$	$\overline{C}_D$	$\overline{C}_L$	$\overline{St}$
0.50	0.924	0.045	1.282	0.034	1.298	0.064	1.323	0.090	-	-	-
0.45	0.926	0.060	1.242	0.054	1.245	0.090	1.311	0.102	-	-	-
0.40	0.922	0.074	1.145	0.084	1.187	0.116	-	-	1.416	0.132	0.200
0.35	0.931	0.092	0.929	0.078	1.031	0.132	-	-	1.451	0.032	0.200
0.30	0.930	0.117	0.941	0.111	0.954	0.164	-	-	1.433	-0.015	0.200
0.25	0.933	0.144	0.951	0.154	0.956	0.198	-	-	1.458	-0.002	0.200
0.20	0.939	0.177	0.954	0.188	-	-	-	-	1.409	0.015	0.167
0.15	0.952	0.231	0.957	0.247	-	-	-	-	1.314	0.043	0.150
0.10	0.958	0.308	0.953	0.306	-	-	-	-	1.114	0.387	0.133
0.05	0.965	0.429	0.941	0.477	-	-	-	-	0.675	0.415	0.050

Numerical simulations present higher values for drag force as expected since it study a two-dimensional flow an as shown by Nishino (2007), the drag force in this flow configuration must be higher than the ones obtained in three-dimensional cases (for $h/d > 0.40$). Although the numerical code exhibit a delay as regards the lift force trend, it follows the experimental results what means the lift force increases as h/d decreases. This behaviour occurs due to the viscosity effects which causes an additional circulation around the body and a change in the stagnation point providing a positive lift to the cylinder. Thus, it can be noticed that the results obtained numerically agree with the approximately two-dimensional ones obtained by Nishino (2007).

Since the main purpose of this work is to study the vortex shedding suppression a special attention must be given to the last column of Tab. 2 which shows the Strouhal number proceeding as the cylinder comes close to the ground. It can be noted from Tab. 2 a decrease in Strouhal number (consequently a decrease in vortex shedding) as h/d decreases. In order to explain the causes of this reduction the analysis is focused on two gap-ratios: $h/d = 0.35$ and $h/d = 0.05$.

Figure 2 shows the time evolution of the aerodynamic forces for the two gap-ratios mentioned above. In order to study in detail the physics involved on vortex shedding suppression five points are highlighted in the charts.

When the distance between the cylinder and the ground is $h/d = 0.35$ the same sequence of events described for the isolated circular cylinder occurs (see Bimbato *et al*. (2011)). However it can be seen in drag curve (Fig. 2(a)) peaks sometimes bigger, sometimes smaller; this happens due to the third mechanism that governs the ground effect phenomenon: the blockage effect imposed by the ground surface. The upper vortex structure has total freedom to grow up to be fully incorporated by the viscous wake (see, in the sequence, Figs. 3(a), 3(b), 3(c) and 3(d)), which results in bigger peaks in the drag force (see Fig. 2(a)). On the other hand, the growth of the lower vortex structure is limited by the ground surface when this vortex structure is been incorporated by the viscous wake (see, in the sequence, Figs. 3(c), 3(d), 3(a) and 3(b)), which causes smaller peaks in the drag force (see Fig. 2(a)).

Figure 2(b) shows the time evolution of the aerodynamic forces acting on the circular cylinder when it is $h/d = 0.05$ away from the moving ground. It can be noted that the periodic and alternate vortex shedding almost disappears for this gap-ratio (see the Strouhal number in Tab. 2). Since the body is too close to the ground the viscosity effects and the Venturi effect work together to cause radical changes in the aerodynamic behaviour of the circular cylinder.

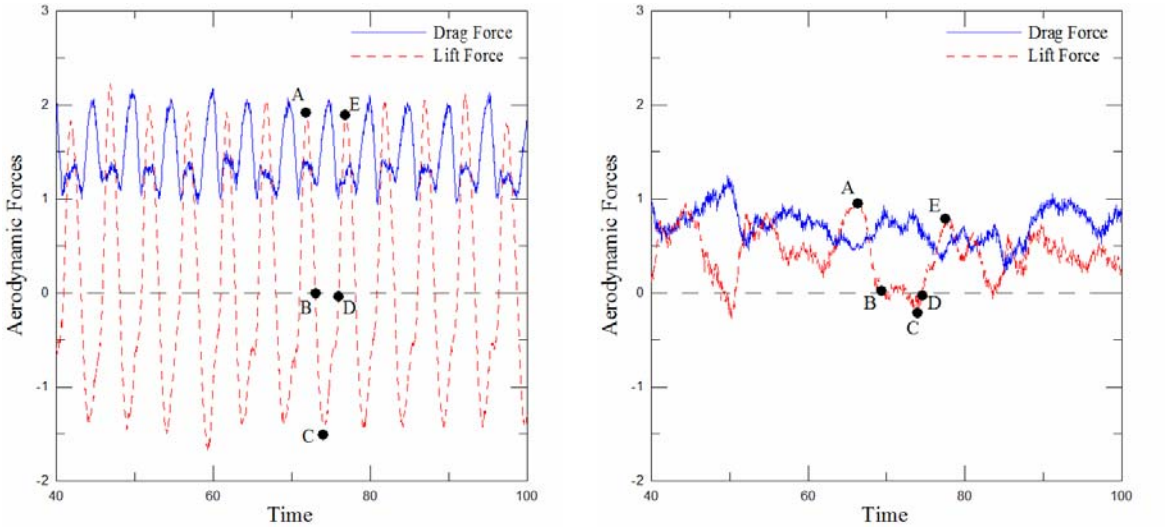

(a) h/d = 0.35 (b) h/d = 0.05

Figure 2. Time evolution of the aerodynamic loads for a circular cylinder in ground effect.

The viscosity effects generate an additional circulation around the body and a great change in the stagnation point (see Fig. 4) providing a high lift force to the cylinder (for $h/d = 0.05$, $\overline{C}_L = 0.415$). Compare the pressure distribution at instants represented by point A in Figs. 4(a) and 4(b) to see how the stagnation point moves downstream.

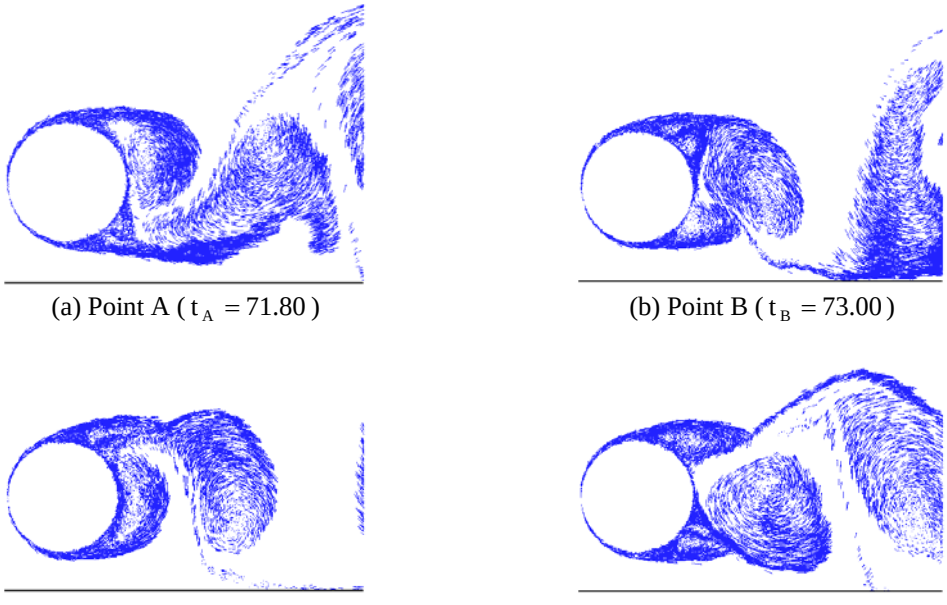

(a) Point A ($t_A = 71.80$) (b) Point B ($t_B = 73.00$)

(c) Point C ($t_c = 74.00$) (d) Point D ($t_D = 75.95$)

Figure 3. Near field velocity distribution for a circular cylinder in ground effect ($h/d = 0.35$).

On the other hand the great Venturi effect contribution is to draw the counter-clockwise vortex structure downstream; as consequence the clockwise vortex structure detachment and its incorporation by the viscous wake is delayed (compare Figs. 3(c) and 3(d) with Figs. 5(c) and 5(d)). Due to delay in clockwise vortex structure detachment the counter-clockwise vortex structure becomes larger causing a deformation in the next clockwise vortex structure that is borning at the instant represented by point A (compare Fig. 3(a) with Fig. 5(a)). As this clockwise vortex structure is growing deformed it does not have enough energy to attract the lower shear layer at this moment. In fact the upper vortex structure is fed by the large counter-clockwise vortex structure; when the upper structure grows enough it causes the counter-clockwise vortex structure detachment and its incorporation by the viscous wake (see Fig. 5(b). Thus the proximity between the body and the ground modify all the mechanism of vortex shedding causing its suppression as can be seen by the Strouhal number (compare the Strouhal number values for $h/d = 0.35$ and $h/d = 0.05$ in Tab. 2).

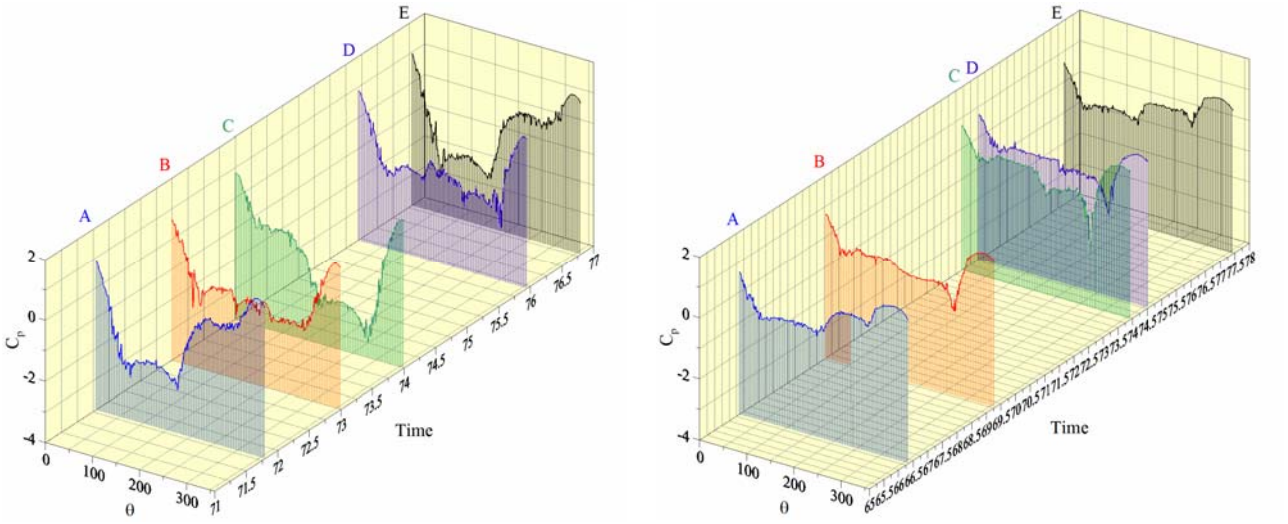

(a) h/d = 0.35 (b) h/d = 0.05

Figure 4. Instantaneous pressure distribution for a circular cylinder in ground effect.

When the gap-ratio is $h/d = 0.05$ it is difficult to define the exact moment of the clockwise vortex structure birth (see again, Fig. 2(b) and compare Fig. 5(a) with Figs. 3(a)). Since the Venturi effect is strong it takes a relatively long time until the counter-clockwise vortex structure birth (compare the time it takes from point *A* to point *C* in Figs. 2(a) and 2(b)). During this time the clockwise vortex structure grows overmuch (see Fig. 5(b)); as consequence the counter-clockwise vortex structure is almost all confined by the presence of the ground and the larger clockwise vortex structure (see Fig. 5(c)). Once the counter-clockwise vortex structure is confined it starts to feed the clockwise vortex structure until its detachment (see Fig. 5(d)). As soon as starts the clockwise vortex structure detachment the counter-clockwise structure begins to go through the space formed between the ground and the upper vortex structure (see Figs. 5(d) and 5(a)).

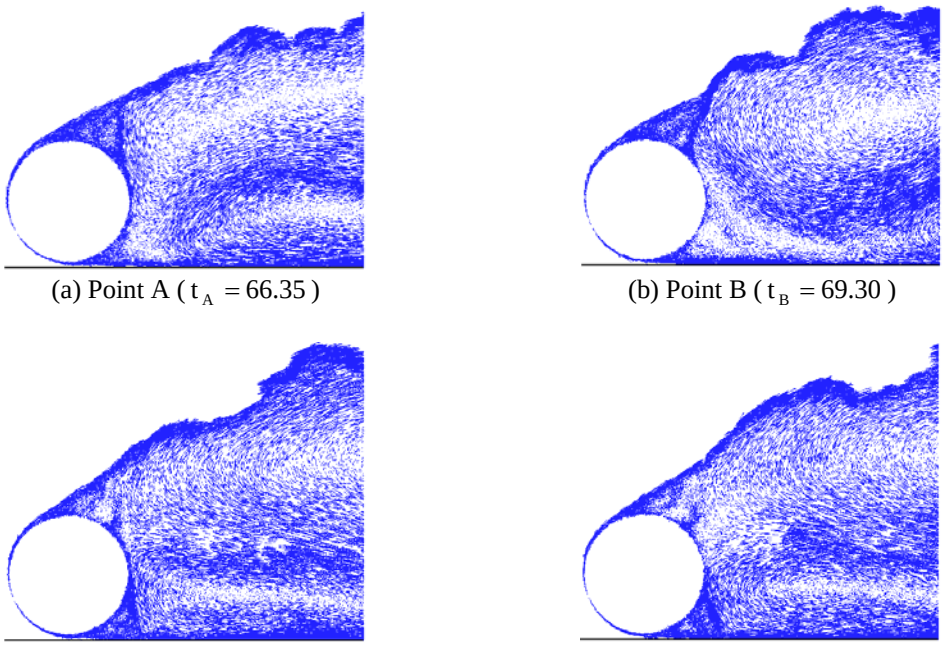

(a) Point A ($t_A = 66.35$) (b) Point B ($t_B = 69.30$)

(c) Point C ($t_C = 73.95$) (d) Point D ($t_D = 74.55$)

Figure 5. Near field velocity distribution for a circular cylinder in ground effect ($h/d = 0.05$).

As it can be seen, the vortex shedding still exists but it is weaker and delayed. In fact due to Venturi Effect the interaction between the upper and lower structures which is a necessary condition for the vortex structures detachment is weakened causing a decrease in drag force as h/d decreases (Tab. 2). Although the total vortex shedding suppression has not been captured it is expected that it will happen as the body comes closer to the moving ground. Figure 6 shows the vortex shedding suppression effect development as the gap-ratio decreases.

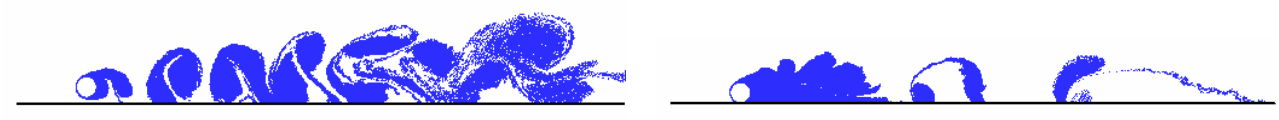

(a) $h/d = 0.35$ (b) $h/d = 0.05$

Figure 6. Position of discrete vortices in the wake of a circular cylinder in ground effect until position $x = 25$.

5. CONCLUSIONS

The vortex code developed in this work represented successfully the vortex shedding suppression which occurs when a circular cylinder is placed near a moving ground. The numerical strategy used to represent the ground plane motion is particular important to save CPU time and it is shown its ability to study relative motion. The numerical results agree well with the experimental ones obtained by Nishino (2007) and show that the Venturi effect in addition with the viscous effects are the responsible for the decrease on drag force and the increase on lift force as the cylinder comes close to the moving ground. It is shown that the ground effect phenomenon is governed by three mechanisms: the wake interference effect, the three-dimensional effects and the blockage effect. The numerical simulations presented in this work are an initial study of the vortex shedding suppression. In a near future, it will be study the wake interference effect which was despised in this work; besides, the study of the flow around an aerodynamic profile placed near a fixed ground and near a moving ground will be considered. Finally, the roughness effects are under development.

6. ACKNOWLEDGEMENTS

This work was supported by CNPq (Proc. 142804/2008-8) and FAPEMIG (Proc. TEC-APQ-01070-10 and Proc. PCE-00551-12).

7. REFERENCES

Batchelor, G. K., 1967. An Introduction to Fluid Dynamics, Cambridge University Press.

Bearman, P. W., Zdravkovich, M. M., 1978. Flow around a Circular Cylinder near a Plane Boundary. Journal of Fluid Mechanics, vol. 89, pp. 33-47.

Bimbato, A. M., Alcântara Pereira, L. A., Hirata, M. H., 2011. Study of the Vortex Shedding Flow around a Body near a Moving Ground. Journal of Wind Engineering and Industrial Aerodynamics, vol. 99, pp. 7-17.

Blevins, R. D., 1984. Applied Fluid Dynamics Handbook. Van Nostrand Reinhold Co..

Buresti, G., Lanciotti, A., 1979. Vortex Shedding from Smooth and Roughened Cylinders in Cross-Flow near a Plane Surface. Aeronautical Quarterly, vol. 30, pp. 305-321.

Chorin, A. J., 1973. Numerical Study of Slightly Viscous Flow. Journal of Fluid Mechanics, vol. 57, pp. 785-796.

Ferziger, J. H., 1981. Numerical Methods for Engineering Application, John Wiley & Sons Inc..

Kamemoto, K., 1993. Procedure to Estimate Unsteady Pressure Distribution for Vortex Method (In Japanese). Trans. Jpn. Soc. Mech. Eng., vol. 59, n. 568 B, pp. 3708-3713.

Kamemoto, K., 2004. On Contribution of Advanced Vortex Element Methods toward Virtual Reality of Unsteady Vortical Flows in the New Generation of CFD. J. Braz. Soc. Mech. Sci. & Eng., vol. 26, n. 4, Rio de Janeiro, Oct. / Dec..

Katz, J., Plotkin, A., 1991. Low Speed Aerodynamics: From Wing Theory to Panel Methods. McGraw Hill, Inc..

Leonard, A., 1980. Vortex Methods for Flow Simulation. Journal of Computational Physics, vol. 37, pp. 289-335.

Lewis, R. I., 1991. Vortex Element Method for Fluid Dynamic Analysis of Engineering Systems. Cambridge Univ. Press, Cambridge, England, U.K..

Nishino, T., 2007. Dynamics and Stability of Flow past a Circular Cylinder in Ground Effect. Ph.D. Thesis, Faculty of Engineering Science and Mathematics, University of Southampton.

Sarpkaya, T., 1989. Computational Methods with Vortices – The 1988 Freeman Scholar Lecture. Journal of Fluids Engineering, vol. 111, pp. 5-52.

Shintani, M., Akamatsu, T., 1994. Investigation of Two-Dimensional Discrete Vortex Method with Viscous Diffusion Model. CFD Journal, vol. 3, n. 2, pp. 237-254.

Taneda, S., 1965. Experimental Investigation of Vortex Streets. Journal of the Physical Society of Japan, vol. 20, pp. 1714-1721.

Uhlman, J. S., 1992. An Integral Equation Formulation of the Equation of an Incompressible Fluid. Naval Undersea Warfare Center, T.R. 10-086.

8. RESPONSIBILITY NOTICE

The authors are the only responsible for the printed material included in this paper.